

# ACSS2/AMPK/PCNA pathway-driven proliferation and chemoresistance of esophageal squamous carcinoma cells under nutrient stress

LEI MI<sup>1\*</sup>, YUEPENG ZHOU<sup>1\*</sup>, DAN WU<sup>1</sup>, QING TAO<sup>1</sup>, XUEFENG WANG<sup>2</sup>, HAITAO ZHU<sup>3</sup>, XINGYU GAO<sup>1</sup>, JINGZHI WANG<sup>1</sup>, RUI LING<sup>1</sup>, JING DENG<sup>4</sup>, CHAOMING MAO<sup>1,5</sup> and DEYU CHEN<sup>1</sup>

<sup>1</sup>Institute of Oncology, <sup>2</sup>Central Laboratory, <sup>3</sup>Department of Medical Imaging, Affiliated Hospital of Jiangsu University; <sup>4</sup>School of Medicine, Jiangsu University; <sup>5</sup>Department of Nuclear Medicine, Affiliated Hospital of Jiangsu University, Zhenjiang, Jiangsu 212001, P.R. China

Received April 1, 2019; Accepted August 8, 2019

DOI: 10.3892/mmr.2019.10735

**Abstract.** Although platinum-based chemotherapy is the first-line choice for locally advanced or metastatic esophageal squamous cell carcinoma (ESCC) patients, accelerated recurrence and chemoresistance remain inevitable. New evidence suggests that metabolism reprogramming under stress involves independent processes that are executed with a variety of proteins. This study investigated the functions of nutrient stress (NS)-mediated acetyl-CoA synthetase short-chain family member 2 (ACSS2) in cell proliferation and cisplatin-resistance and examined its combined effects with proliferating cell nuclear antigen (PCNA), a key regulator of DNA replication and repair. Here, it was demonstrated that under NS, when the AMP-activated protein kinase (AMPK) pathway was activated, ESCC cells maintained proliferation and chemoresistance was distinctly upregulated as determined by CCK-8 assay. As determined using immunoblotting and RT-qPCR, compared with normal esophageal epithelial cells (Het-1A), ESCC cells were less sensitive to NS and showed increased intracellular levels of ACSS2. Moreover, it was shown that ACSS2 inhibition by siRNA not only greatly interfered with proliferation under NS but also participated in DNA repair after cisplatin treatment via PCNA suppression, and the acceleration of cell death was dependent on the activation of the

AMPK pathway as revealed by the Annexin V/PI and TUNEL assay results. Our study identified crosstalk between nutrient supply and chemoresistance that could be exploited therapeutically to target AMPK signaling, and the results suggest ACSS2 as a potential biomarker for identifying higher-risk patients.

## Introduction

Proliferating cell nuclear antigen (PCNA) is a clamp homotrimer that encircles mammalian DNA as a scaffold and is overexpressed in various types of cancer; thus, PCNA participates in DNA replication, DNA damage repair and cell cycle regulation and plays a critical role in anti-apoptosis, chromatin metabolism and gene expression (1,2). Notably, the importance of PCNA in DNA repair, as revealed by a subset of methods, including homologous recombination, nucleotide excision repair, mismatch repair and translesion DNA synthesis, have revealed the importance of PCNA in DNA repair, recruiting various repair factors to disrupt the DNA damage from chemotherapy treatments, such as platinum-based drugs (2,3). The overexpression of PCNA in tumors is often associated with the maintenance of aggressiveness and the stimulation of excessive proliferation by providing the genomic material, which is necessary for cell division and genomic integrity (4-6). Given the essential function of PCNA in cancer or normal cells, whose functions mostly depend on posttranslational modifications, an intricate network of associated proteins and signaling molecules may exist, but the key factors or exact mechanisms that mediate its expression are not understood (1).

One possible approach that may provide insightful and valuable information is examining the tumor microenvironment. Previous studies have established that limited nutrient supply or rather nutrient stress (NS), a common but distinguished feature, is also an important stimulus of proliferation, antagonism, survival and metastasis for different cancer types (7-13). The excessive nutrient consumption hinders cell division, and the metabolic phenotype makes cancer cells more sensitive to hypoxia and nutrient starvation (14,15). The abnormal metabolism of multiple tumors confers the ability to utilize other metabolic substances represented by acetate (16,17). In light

---

*Correspondence to:* Professor Deyu Chen or Professor Chaoming Mao, Institute of Oncology, Affiliated Hospital of Jiangsu University, 438 Jiafang Road, Jiangkou, Zhenjiang, Jiangsu 212001, P.R. China  
E-mail: cdeyu@hotmail.com  
E-mail: jq1001@ujs.edu.cn

\*Contributed equally

*Abbreviations:* ESCC, esophageal squamous cell carcinoma; NS, nutrient stress; ACSS2, acetyl-CoA synthetase short-chain family member 2; PCNA, proliferating cell nuclear antigen

*Key words:* ACSS2, esophageal squamous cell carcinoma, PCNA, chemoresistance, AMPK

of restricted resources resulting in stress, cancer cells convert acetate to acetyl-CoA and other various biomolecules and energy sources to support cellular activity, particularly proliferative or metastatic activity (18-20). Acetyl-CoA synthetase short-chain family member 2 or acetyl-CoA synthetase 2 (ACSS2) is responsible for the production of acetyl CoA from acetate, and recent research has uncovered its differential and even conflicting roles in proliferation, fatty acid synthesis, metastasis and chemoresistance (14,20-24). Moreover, the role of ACSS2 in metabolism reprogramming and further signal transmission, especially under NS, has only sparsely been investigated.

New evidence suggests that beyond classical resistance mechanisms, microenvironment stress also results in antagonism-independent alterations of the drug target, overactive DNA repair and survival pathways, enhanced expression of detoxification proteins and drug efflux (25,26). In coping with drug-induced double-strand breaks (DSBs), cancer cells rapidly initiate the DNA damage response (DDR) to ensure the efficient and accurate repair of damaged DNA and cell survival. Before initiating repair, the phosphorylation and position of H2AX with the recruitment of PCNA in the DNA breaks provide a docking site for other DNA repair factors. Among these factors, ataxia telangiectasia mutated (ATM) and DNA-dependent protein kinase catalytic subunit (DNA-PKcs) are two primary kinases that phosphorylate H2AX at S139 in response to DSBs (1,3,27). Although multiple signaling transduction pathways are involved in the activation and transcriptional regulation, targeting AMP-activated protein kinase (AMPK) activation, yet as a double-edged sword, is worth exploring (28-31). Moreover, studies have reported that PCNA expression is affected by AMPK, a master nutrient sensor that is imbalanced in several types of cancer, yet the physiological implications of the PCNA and AMPK interaction, especially under NS, are poorly understood (32-36). Elucidation of the metabolic alterations during the progression of cancer may offer potential therapeutic targets for the challenge of chemoresistance. The present study investigated the impact of ACSS2 on chemoresistance under NS and sought a more complete understanding of the underlying mechanisms between the AMPK pathway and PCNA in DNA repair, beyond its role in proliferation.

## Materials and methods

**Cell lines and reagents.** ESCC cell lines TE-1 and ECA-109 were purchased from The Cell Resource Centre of Shanghai Institutes for Biological Sciences, Chinese Academy of Science (Shanghai, China) and cultured in RPMI-1640 medium (Gibco; Thermo Fisher Scientific, Inc., China) supplemented with 10% dialyzed fetal bovine serum (FBS; Biological Industries, Kibbutz Beit-Haemek, Israel), 1% compound antibiotics (Pen Strep; Gibco; Thermo Fisher Scientific, Inc.). Immortalized human normal esophageal epithelial cells, Het-1A (purchased from BeNa Culture Collection, Kunshan, Jiangsu, China), were maintained in DMEM (Gibco; Thermo Fisher Scientific, Inc., China), supplemented with 10% FBS as described previously (37). For induction of nutrient starvation, ESCC cells (ESCCs) or Het-1A cells (confluence of 50-60%) were transferred to serum lacking media (supplemented

with 1% FBS) for the indicated periods of time. Cells were tested negative for mycoplasma or other infectious agents, and maintained at 37°C in a humidified atmosphere with 5% CO<sub>2</sub>. ACSS2 (cat. no. sc-398559; Santa Cruz Biotechnology, Santa Cruz, CA, USA), ATM (product #2873)/p-ATM (product #5883), BRCA1 (product #9010)/p-BRCA1 (product #9009), Bcl-xL (product #2762),  $\gamma$ H2AX (product #9718), DNA-PKcs (product #4602), ULK1 (product #8054)/p-ULK1 (product #5869), AMPK (product #5831)/p-AMPK (product #50081), PCNA (product #2586), Ki-67 (product #9449) and  $\beta$ -actin (product #58169) (Cell Signaling Technology, Danvers, MA, USA), Bax (catalog no. AF0120; Affinity, Changzhou, China), Lipofectamine 2000 (Invitrogen; Thermo Fisher Scientific, Inc.), and dorsomorphin (an inhibitor of the AMPK pathway; APEX BIO, USA) were used following the manufacturer's instructions.

**Patients and specimens.** Cancer tissues and paired normal tissues were obtained from 28 patients with ESCC at the Affiliated Hospital of Jiangsu University (Zhenjiang, China) from 2010 to 2018. The Ethics Committee of the Affiliated Hospital of Jiangsu University approved the research. Firstly, the ESCC samples were confirmed by the Pathology Department, and then serial sections were processed and stained with anti-ACSS2 (1:200 dilution; cat. #sc-398559; Santa Cruz Biotechnology), anti-Ki-67 (1:1,000 dilution; product #9449, Cell Signaling Technology) and anti-PCNA (1:4,000 dilution; product #2586, Cell Signaling Technology) antibodies for the immunohistochemistry (IHC) assay. Ki-67 scores ranged from 0 to 100% as the percentage of positive cells within the area of invasive cells. The evaluation criteria for ACSS2 or PCNA were based on our previously published study (13). The proportion of positively staining tumor cells and the staining intensity were examined and scored by five independent pathologists, who were blinded to the patient clinical information as previously described (13). All methods, including the collection and use of patient samples, were performed in accordance with the relevant guidelines and regulations and all patients provided signed informed consent.

**RNA interference and plasmid infection.** Knockdown of human ACSS2 and PCNA were performed using gene-specific siRNAs. These gene-specific siRNA and including control siRNA were purchased from Shanghai GenePharma (Shanghai GenePharma Co., Ltd., Shanghai, China), which were reconstituted in sterile DEPC water to a stock concentration of 20  $\mu$ M, and transfected into TE-1 and ECA-109 cells using Lipofectamine 2000. The siRNA sequences were as follows: siRNA-ACSS2: Sense, 5'-UAUGCUUGGUGACAG GCUCAUCC-3' and antisense, 5'-GGAGAUGAGCCU GUCACCAAGCAUA-3'; siRNA-PCNA: Sense, 5'-UAUGGU AACAGCUUCCUCCTT-3' and antisense, 5'-GGAGGAAGC UGUUACCAUATT-3'. The inhibitory effect of the siRNA transfection was evaluated with RT-qPCR and western blotting. Upregulation of ACSS2 expression was performed by cloning ACSS2 full-length complementary DNA into a GV141 carrier plasmid, including the control plasmid group, which were purchased from Shanghai Genechem Co., Ltd. (Shanghai, China), and these plasmids were transfected

into TE-1 and ECA-109 cells using Lipofectamine 2000. The upregulation effect of the plasmid was evaluated with RT-qPCR and western blotting. After transfection, the cells were subjected to other treatments for the indicated duration and then used for the subsequent assays.

**Quantitative real-time polymerase chain reaction (qPCR).** RNA was extracted using RNAiso Plus in accordance with the manufacturer's instructions and reverse transcribed into cDNA using a reverse transcription reagent kit, according to the manufacturer's protocol (both from Takara Biotechnology Co., Ltd., Dalian, China). The RT-PCR reactions were prepared using a PCR kit (Takara Biotechnology Co., Ltd.) and performed on an Agilent Mx3000P™ Real-Time PCR System (Stratagene). The primers used were synthesized by Invitrogen (Invitrogen; Thermo Fisher Scientific, Inc.), and the sequences were as follows: ACSS2 primers, 5'-GGATTCCAGCTGCAGTCTTC-3' (forward) and 5'-CAGCCAGCTCCTTCAGGTT-3' (reverse); PCNA primers, 5'-CTGAAGCCGAAACCAGCTAGACT-3' (forward) and 5'-TCGTTGATGAGGTCCTTAGTGC-3' (reverse);  $\beta$ -actin primers, 5'-TCACCCACTGTGCCATCTACGA-3' (forward) and 5'-CAGCGGAACCGCTCATTGCCAATGG-3' (reverse). Relative expression levels were calculated using the  $2^{-\Delta\Delta C_q}$  method (38) and  $\beta$ -actin was used as an internal reference gene.

**Immunoblotting.** Cells of different treatment were collected by centrifugation with 1200 rpm in 5 min, processed and lysed in RIPA buffer supplemented with a protease inhibitor cocktail and PMSF (all purchased from Beijing Solarbio Science & Technology Co., Ltd., Beijing, China) according to the manufacturer instructions. Protein concentration was determined by BCA protein assay (CoWin Biotech Co., Ltd, Beijing, China), and 5  $\mu$ l of protein were loaded and separated by 8 to 12% SDS-PAGE. After transfer to PVDF membranes, 5% BSA in TBST was used to block the membrane at room temperature for 1 h. The membranes were incubated with primary antibodies [ACSS2 (at 1:2,000 dilution); ATM, p-ATM, BRCA1, p-BRCA1, Bcl-xL,  $\gamma$ H2AX, DNA-PKcs, ULK1, p-ULK1, AMPK, p-AMPK, PCNA, and Ki-67 (at 1:1,000 dilution);  $\beta$ -actin (at 1:2,000 dilution); Bax (at 1:500 dilution)] saturated with 5% BSA in TBST at 4°C overnight. On the next day, the membranes were incubated with HRP-conjugated anti-rabbit or -mouse antibody (at 1:5,000 dilution, product #7074 and #7076; Cell Signaling Technology) for 1 h at room temperature, and then exposed to enhanced ECL reagent (Nanjing Vazyme Biotech Co., Ltd., Nanjing, China), imaged by an automatic Chemiscope-4300 imager (Clinx Science Instruments Co., Ltd., Shanghai, China) and data were analyzed with Fluor Chem FC3 software (Protein-Simple, USA).

**CCK-8 assay.** Cell proliferation was examined using the CCK-8 Cell Counting Kit (Nanjing Vazyme Biotech Co., Ltd.) according to the manufacturer's instructions. Briefly, TE-1/ECA-109 and Het-1A cells were grown in a 96-well plate for 24 h, transfected with siRNA-ACSS2 or the negative control, and then cultured in normal medium or under NS. To measure the cell proliferation at 0, 24, 48, or 72 h after transfection, 10  $\mu$ l of CCK-8 was added to each well for 1 h.

Absorbance was measured at a wavelength of 450 nm by a microplate reader (BioTek, USA). Assays were repeated at least three times.

**Flow cytometric analysis.** The effect of ACSS2 on cell cycle distribution was determined by flow cytometry. Briefly, cells subjected to the indicated treatments were harvested when they reached 80% confluence, washed with PBS and resuspended in 1 ml of DNA staining solution and 10  $\mu$ l of permeabilization solution (MultiSciences Biotech Co., Ltd., Hangzhou, China). Following incubation for 30 min in the dark at room temperature, the cells were analyzed by flow cytometry at 72 h after interference. The fractions of cells in the G0/G1, S, and G2/M phases were analyzed. Cell apoptosis was detected using an Annexin V-FITC/PI Apoptosis Detection kit (MultiSciences Biotech Co., Ltd., Hangzhou, China) according to the supplier's protocol. Cells were seeded in 12-well plates (6x10<sup>4</sup>/well). The cells were harvested after transfection with siRNA or NC and with or without DDP (5  $\mu$ g/ml) treatment for 24 h, and washed in cold PBS. Then, cells were resuspended in 500  $\mu$ l of binding buffer. Next, 5  $\mu$ l of Annexin V-FITC and 10  $\mu$ l of PI working solution were added to each reaction system at room temperature for 5 min. Flow cytometric analysis was performed immediately on a flow cytometer (BD FACSCanto II; BD Biosciences) and data were analyzed with BD FACSDiva software (BD Biosciences). Each experiment was repeated at least three times.

**TUNEL staining and immunofluorescence.** After pretreatment with siRNA or NC, and with or without DDP (5  $\mu$ g/ml) for the indicated time, ESCC monolayers were spun down on slides, and stained by a TUNEL Apoptosis Detection kit (#A113-01; Nanjing Vazyme Biotech Co., Ltd., Nanjing, China) for in situ detection of apoptosis according to the manufacturer's instructions. In brief, slides were further incubated in the prescribed mixture of enzyme and label solution, at 37°C for 1 h in a humidified chamber. The TUNEL-stained cells were counterstained with PBS containing 4',6-diamidino-2-phenylindole (DAPI, 5  $\mu$ g/ml) (#422801, BioLegend, USA) for 5 min, and counted to calculate the TUNEL indices. For immunofluorescence, after being washed 3 times with PBS and fixed with 4% paraformaldehyde, the cells were permeabilized with 0.5% Triton X-100 in PBS for 10 min. The fixed cells were blocked in 5% BSA in PBS for 1 h at room temperature and incubated with primary antibodies against  $\gamma$ H2AX (at 1:400 dilution; product #9718, Cell Signaling Technology), p-ATM (at 1:500 dilution; product #5883, Cell Signaling Technology) and PCNA (at 1:2,000 dilution; product #2586, Cell Signaling Technology) overnight at 4°C. FITC-conjugated anti-mouse, Cy3-conjugated anti-rabbit secondary antibodies (1:100 dilution; cat. #SA00003 and #SA00009, Proteintech Group, Wuhan, China) were used to detect the bound primary antibody. Then, the slides were washed 3 times in PBS and incubated with DAPI for 5 min. Immunofluorescence results are representatives of at least three independent experiments. Images were captured on a fluorescence (BX51, Olympus, Japan) or laser confocal microscope (LSM800, ZEISS, Germany) with fixed settings between samples and analyzed using ImageJ software (National Institutes of Health, Bethesda, MD, USA).

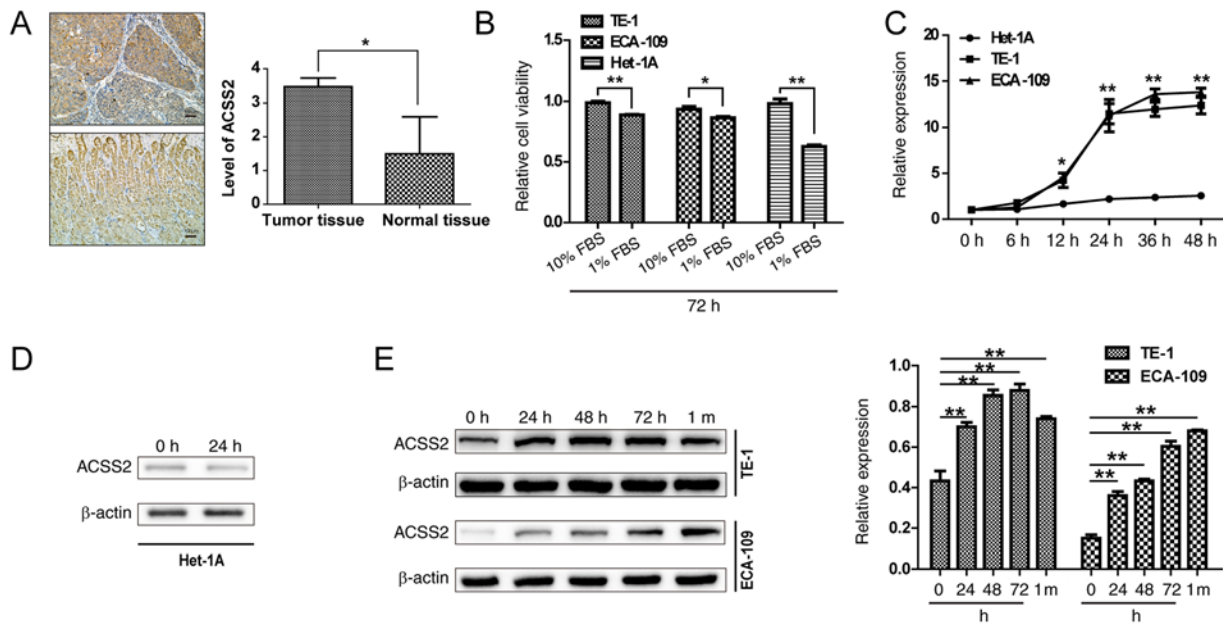


Figure 1. ESCC cells are more sensitive to nutrient stress with increased ACSS2 expression. (A) Typical IHC images of ACSS2 in human ESCC tumor tissue (upper panel) and paracancerous normal tissue (lower panel; scale bar, 100  $\mu$ m). The level of ACSS2 in tumor and normal tissues (left histogram). (B) ESCC cells (TE-1 and ECA-109) and human esophageal squamous epithelial cells (Het-1A) were cultured in medium containing only 1 or 10% FBS for the indicated time, and then subjected to CCK-8 assays. (C) RNA samples were used to determine the levels of ACSS2 mRNA in Het-1A and ESCC cells cultured under nutrient stress or not at the indicated periods by RT-PCR. (D) The protein lysates of Het-1A cells under nutrient stress or not for 24 h were subjected to western blotting. (E) Western blotting was conducted to detect expression of ACSS2 in TE-1 and ECA-109 cells under nutrient stress at the indicated periods (left panel).  $\beta$ -actin was used as a loading control. Bar chart shows the expression ratios of ACSS2 to  $\beta$ -actin (right panel). Data are mean  $\pm$  SEM of three independent experiments. h, hour; m, month; \* $P$ <0.05, \*\* $P$ <0.001. IHC, immunohistochemistry; ESCC, esophageal squamous cell carcinoma; ACSS2, acetyl-CoA synthetase short-chain family member 2.

**Statistical analysis.** All experimental data are presented as the means  $\pm$  standard deviation (SD) from three independent experiments. Survival curves were generated by Kaplan-Meier analysis and tested for significance using the Breslow test. The  $\chi^2$ -test was used to explore the relationship between two variables. The differences between two groups were analyzed using Student's *t*-test, and comparisons in datasets containing multiple groups were analyzed using one-way analysis of variance (ANOVA) followed by the Newman-Keuls post-test. Significant differences were determined using a threshold *P*-value of 0.05.

## Results

**ESCCs are more sensitive to NS, and are associated with increased expression of ACSS2.** IHC staining analysis was used to measure ACSS2 expression in 28 pairs of human ESCC and adjacent normal tissues, and the results revealed that ACSS2 exhibited positive cytoplasmic staining. In cancer tissues, ACSS2 protein was highly expressed in central zones and hypercellular areas, while ACSS2-positive cells in adjacent noncancerous tissues were concentrated in stroma cells and the glandular epithelium at basal and lower levels (Fig. 1A). To investigate the potential role of NS caused by excessive proliferation or poor nutrient supply, we first examined the effect of limited serum on cell viability. As shown in Fig. 1B, the proliferation of TE-1 and ECA-109 cells was significantly decreased at 72 h after the replacement of both media with 1% FBS (NS;  $P$ =0.008 and 0.03), while the proliferation of Het-1A cells was decreased more significantly ( $P$ <0.01), suggesting that normal

esophageal epithelial cells are more sensitive to nutrient supply. To study the role of ACSS2 in the adaptive mechanisms of ESCCs to NS, the transcription levels of ACSS2 were analyzed at different times in limited serum medium. ACSS2 expression showed a sharp increase at 12 h in the TE-1 and ECA-109 cells compared to that in the Het-1A cells ( $P$ =0.03) under NS. The mRNA levels reached 9- to 12-fold at 24 h ( $P$ <0.01), and the expression levels of ACSS2 mRNA in the TE-1 and ECA-109 cells tended to reach a plateau after 24 h, but the levels were still at a higher level than those in the Het-1A cells ( $P$ <0.01) (Fig. 1C). However, the mRNA and protein expression of ACSS2 in the normal esophageal epithelial Het-1A cells did not correlate at all times or under all conditions (Fig. 1C and D), thus effectively adapting to stress and effectively played an extraordinary role, which has been described as a characteristic of cancer cells. When ACSS2 was analyzed in the ESCC cell lines, it was found that ACSS2 protein was upregulated with an increasing period under NS (Fig. 1E). Similarly, ACSS2 was persistently upregulated under NS for more than 1 month (Fig. 1E). ACSS2 has been shown to be upregulated by glucose, lipid deprivation and hypoxia in different cancer cell lines (14,39,40). Together, these data indicate that the proliferation of ESCCs is less restricted than that of human esophageal squamous epithelial cells in response to low serum culture and that the upregulation of ACSS2 may help maintain ESCC cell survival under NS.

**ACSS2 contributes to the proliferation and DNA repair that are regulated by PCNA.** To elucidate the role of ACSS2 in ESCC cell viability, we first performed siRNA experiments.

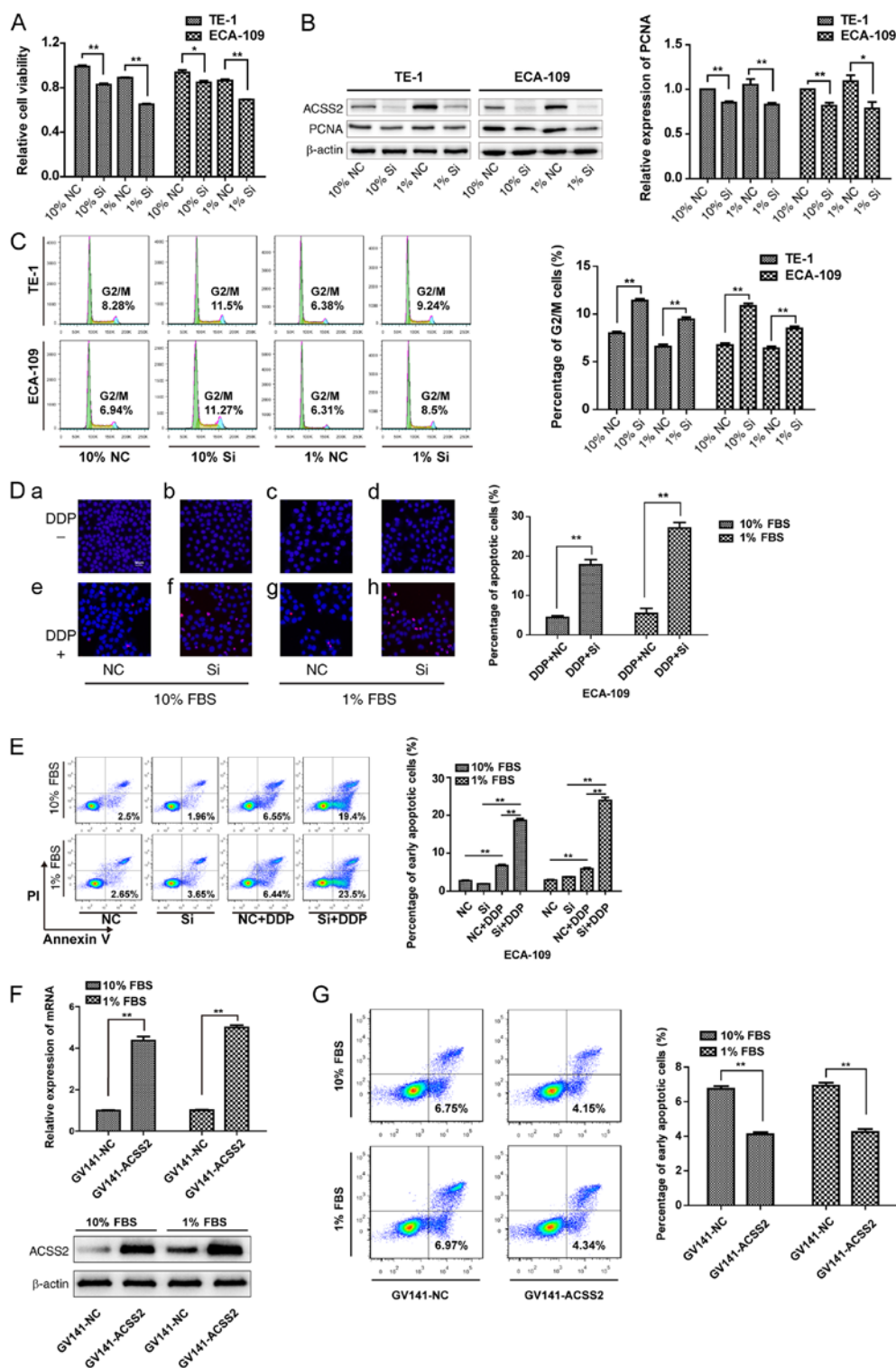


Figure 2. ACSS2 contributes to the proliferation and DNA repair via PCNA. (A) CCK8 assay indicates the cell viability of TE-1 and ECA-109 cells after 72 h post-siRNA transfection (Si) under basal conditions or nutrient stress. (B) The change of PCNA in TE-1 and ECA-109 cells after transfection with siRNA against ACSS2 (Si) or NC under nutrient stress. Bar chart shows the expression ratios of PCNA to  $\beta$ -actin (right panel). (C) Percentages of TE-1 and ECA-109 cells in the G2/M phases by flow cytometry. Histogram shows the percentage of TE-1 and ECA-109 cells in the G2/M phases after 72 h post-siRNA transfection (Si) with or without lower-serum treatment (right panel). (D) Representative images of TUNEL staining. Magnification,  $\times 400$ . ECA-109 cells ( $2 \times 10^4$ ) were grown on coverslips in 24-well plates and fixed for TUNEL staining as described in Materials and methods. Red represents apoptotic cells while the blue indicates nuclei. TUNEL shows ECA-109 cell apoptosis: (a-d) ECA-109 cells were transfected with siRNA-ACSS2 or NC for 72 h under normal or nutrient stress conditions; (e-h) ECA-109 cells were cultured in medium containing cisplatin (DDP) ( $5 \mu\text{g/ml}$ ) for 24 h after transfected with siRNA-ACSS2 or NC for 48 h with or without serum starvation. (E) Flow cytometry was performed to compare the apoptosis ratio between the cells transfected with siRNA-ACSS2 and NC in medium containing  $5 \mu\text{g/ml}$  DDP or not. The percentage of early apoptotic cells generated in the experiments is indicated beside the flow cytometric histograms. (F) RT-PCR and western blotting were conducted to detect expression of ACSS2 after transfection of the plasmid (GV141-ACSS2) under nutrient stress or not. (G) Flow cytometry was performed to compare the apoptosis ratio between the cells transfected with GV141-ACSS2 and the GV141-NC in medium containing  $5 \mu\text{g/ml}$  cisplatin under nutrient stress or not. The percentage of early apoptotic cells generated in the experiments is indicated beside the flow cytometric histograms. All data are presented as mean  $\pm$  SEM ( $n=3$  or  $4$ ) ( $P<0.05$ ;  $**P<0.01$ ). ACSS2, acetyl-CoA synthetase short-chain family member 2; PCNA, proliferating cell nuclear antigen; Si, siRNA-ACSS2; NC, negative control.

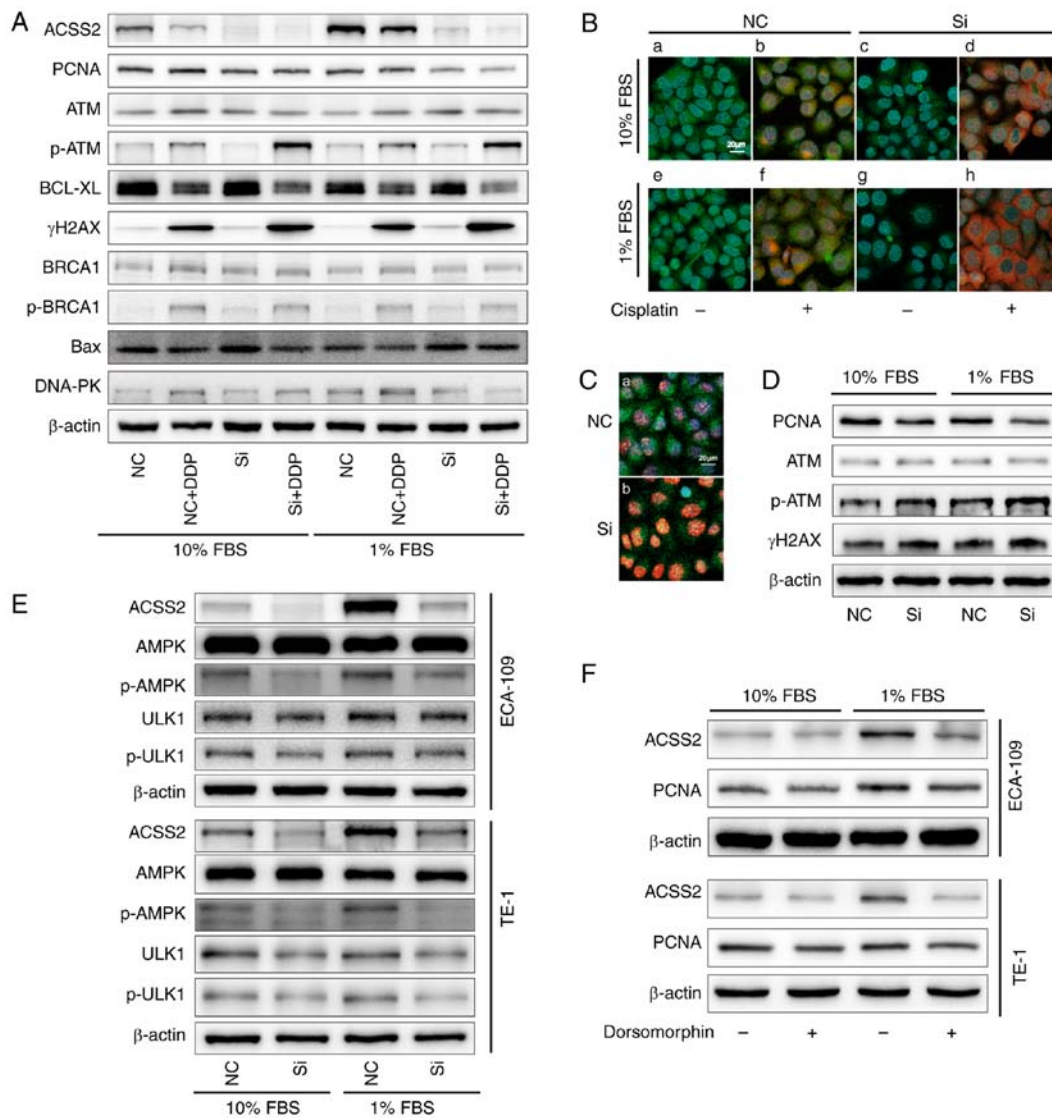


Figure 3. ACSS2/AMPK/PCNA signaling regulates DNA damage response under nutrient stress. (A) ECA-109 cells were grown in different media containing 10% FBS or 1% FBS for 48 h after being transfected with siRNA-ACSS2 (Si) or negative control (NC), then stimulated with cisplatin (DDP) ( $5 \mu\text{g/ml}$ ) for 24 h or replacement, subjected to immunoblotting analysis for the indicated proteins. (B and C) Immunofluorescence. Magnification,  $\times 400$ . ECA-109 cells were treated with cisplatin ( $5 \mu\text{g/ml}$ ) for 24 h after interference for 48 h under basal and stress conditions, then triple-labeled with anti-PCNA (green), anti-phosphorylated ATM (p-ATM) (red in B) or anti- $\gamma\text{H2AX}$  (red in C), and DAPI (blue, nuclei) as shown in the figures. (D) ECA-109 cells were treated with cisplatin for 24 h after being transfected with siRNA against PCNA (Si) for 24 h under normal or nutrient deficiencies. Expression of ATM/p-ATM and  $\gamma\text{H2AX}$  was detected by immunoblotting. (E) Contribution of ACSS2 to the AMPK pathway for cells incubated using complete medium or low-serum medium, as assessed by siRNA-mediated knockdown. (F) Western blot analysis was performed to show the changes in ACSS2 and PCNA in the dorsomorphin-treated groups compared with the NC group. ACSS2, acetyl-CoA synthetase short-chain family member 2; AMPK, AMP-activated protein kinase; PCNA, proliferating cell nuclear antigen; ATM, ataxia telangiectasia mutated; Bcl-xL, B-cell lymphoma-extra large; BRCA1, breast cancer susceptibility gene 1; Bax, Bcl-2 associated X protein; DNA-PK, DNA-dependent protein kinase catalytic subunit;  $\gamma\text{H2AX}$ , phosphorylate H2AX.

Data from Fig. 2B show that the specific siRNA treatment observably decreased the protein levels of ACSS2. CCK-8 assays were performed to investigate cell proliferation. The results showed that suppression of ACSS2 expression significantly affected the proliferation of TE-1 and ECA-109 cells compared to that of the control group (NC), regardless of whether the cells were grown in normal medium or under NS ( $P < 0.05$ , Fig. 2A). As stated above, PCNA acts as a scaffold to recruit proteins for replication, recombination and DNA repair. siRNA-ACSS2 treatment led to a 15 and 18% decrease in PCNA transcript levels which was further decreased 21 and 28% in combination with NS in the TE-1 and ECA-109 cells, respectively. Since PCNA directly

participates in proliferation, these data suggest that ACSS2 reactivated PCNA in both cell lines, especially under NS (Fig. 2B). This was further confirmed by using flow cytometry, demonstrating substantial increases in G2/M phase arrest in both cell lines upon siRNA-ACSS2 treatment; the histogram (right) shows that the percentage of cells in the G2/M phase in the siRNA-ACSS2 group was approximately 1.4-fold higher than that in the NC group under NS or not ( $P < 0.01$ ) (Fig. 2C). Notably, the G2/M DNA damage checkpoint is important for repairing DNA after replication (6,41-43); thus, its defect would lead to apoptosis or death. Most cells under apoptosis preferentially are labeled by TUNEL for fragmented DNA at later stages. To examine whether DNA damage increased after

Table I. Association of the expression of ACSS2 with clinicopathological characteristics of the ESCC patients.

Parameters	ACSS2 expression		P-value
	Low (13)	High (15)	
Age (years)			
<60	5	6	0.9337
≥60	8	9	
Sex			
Male	9	14	0.0968
Female	4	1	
Degree of differentiation			0.1565
Well	3	5	
Moderate	2	6	
Poor	8	4	
Tumor diameter (cm)			0.3903
<5	9	8	
≥5	4	7	
Lymph node metastasis			0.1939
Yes	3	7	
No	10	8	
Tumor grade			0.2556
I-II	8	6	
III-IV	5	9	
PCNA expression			<b>0.0163</b>
Low	8	2	
High	5	13	
Ki-67 expression			<b>&lt;0.01</b>
≤50%	12	3	
>50%	1	12	

Difference is considered significant when  $P < 0.05$  (shown in bold). ESCC, esophageal squamous cell carcinoma; ACSS2, acetyl-CoA synthetase short-chain family member 2; PCNA, proliferating cell nuclear antigen.

siRNA-ACSS2 treatment, TUNEL analysis was performed to determine apoptosis with or without cisplatin (DDP) treatment. At least five viewing fields were utilized to obtain each data point and a representative of three individual dose-dependent experiments is shown. The results showed that there was no difference in the TUNEL-positive cell ratio between the NC group and the siRNA-ACSS2 group in TE-1 or ECA-109 cells, suggesting that the downregulation of ACSS2 did not induce cell death. However, the level of TUNEL-staining was significantly increased on day 3 posttreatment with siRNA-ACSS2 compared with the NC when treated with DDP (10% FBS:  $17.78 \pm 1.16$  vs.  $4.09 \pm 0.89\%$ ; 1% FBS:  $27.14 \pm 1.23$  vs.  $5.45 \pm 1.07\%$ ;  $P < 0.01$ ) (Fig. 2D). Additionally, ACSS2 interference also significantly increased the percentage of early apoptotic cells compared to that in NC groups after DDP treatment, whether under NS or not ( $P < 0.01$ ), but the differences between the siRNA-ACSS2 and NC groups were not statistically significant at 72 h after transfection (Fig. 2E). To further confirm the role of ACSS2 in chemoresistance, plasmid transfection

experiment were performed, and the data from Fig. 2F shows that specific plasmid treatment significantly increased the mRNA and protein levels of ACSS2 ( $P < 0.01$ ). Upregulation of ACSS2 expression reduced the percentage of early apoptotic cells in comparison to the NC groups after DDP treatment under NS or not ( $P < 0.01$ ) (Fig. 2G). These preliminary data indicate that ACSS2 is a factor that maintains DNA stability and may be associated with PCNA expression.

*ACSS2/AMPK signaling stabilizes PCNA expression and regulates the DNA damage response under NS.* To investigate the potential mechanism of ACSS2-dependent ESCC chemoresistance under NS, the levels of PCNA, p-ATM,  $\gamma$ H2AX and related proteins were assessed. The cooperation of ATM protein kinase and DNA-PKcs plays critical roles in the regulation of the DNA damage response and cellular homeostasis (44,45). As expected, among the siRNA-ACSS2 groups, the expression levels of p-ATM increased 4.5-fold under NS combined with DDP compared to 2.0-fold following DDP treatment alone. However, the downregulation of ACSS2 had no significant effects on DNA-PKcs or p-BRCA1 levels. Importantly, we also observed that both siRNA-ACSS2 and DDP influenced the accumulation of  $\gamma$ H2AX, exhibiting obvious synergistic effects under NS. B-cell lymphoma-extra large (Bcl-xL) is a member of the Bcl-2 family, an anti-apoptotic protein in mitochondria that prevents the release of cytochrome *c*. As an apoptosis activator, Bax leads to a loss in membrane potential and the release of cytochrome *c*. Considering that the lower ACSS2 under NS is much more vulnerable to DNA damage, we further detected variations in Bcl-xL and Bax. However, the suppression of ACSS2 expression in the ESCCs had no significant effect on the protein content of Bcl-xL or Bax, whether under sufficient nutrition or deficiency. Interestingly, despite its inhibitory effect on Bcl-xL, the presence of DDP had no influence on Bax expression (Fig. 3A). As shown in Fig. 3B and C, changes in PCNA and p-ATM and  $\gamma$ H2AX foci were detected in the ESCCs, represented by ECA-109 cells, after treatment with cisplatin. In regards to the p-ATM and PCNA signals, although the percentages of p-ATM-positive cells increased steadily after cisplatin, the frequencies of p-ATM foci peaked at 24 h after downregulation of the expression of ACSS2; 89 to 95% of ESCCs with increased p-ATM showed decreased PCNA staining after low-serum culture for 48 h (Fig. 3B). The changes in the  $\gamma$ H2AX signals were similar to those of the p-ATM foci, and the percentages of PCNA were steadily depended on the levels of ACSS2, but the intensity of  $\gamma$ H2AX was stronger at 24 h post damage (Fig. 3C). These data suggest that nuclear-wide  $\gamma$ H2AX expression, p-ATM responses and PCNA expression are related to ACSS2 expression in ESCCs after cisplatin treatment. More importantly, the effective interference of PCNA combined with DDP treatment also increased  $\gamma$ H2AX and p-ATM expression especially during NS (Fig. 3D), indicating that PCNA plays a vital role as a scaffold associated with ACSS2-regulated DNA repair in ESCCs. The formation of PCNA,  $\gamma$ H2AX, and p-ATM in the DNA damage response is related to the activation of the AMPK signaling pathway in multiple cancer cells (1,46,47). Similarly, our results showed that the significant phosphorylation of AMPK was induced by culture of TE-1 and ECA-109 cells under NS. The inhibition of ACSS2 accompanied by the significant downregulation of

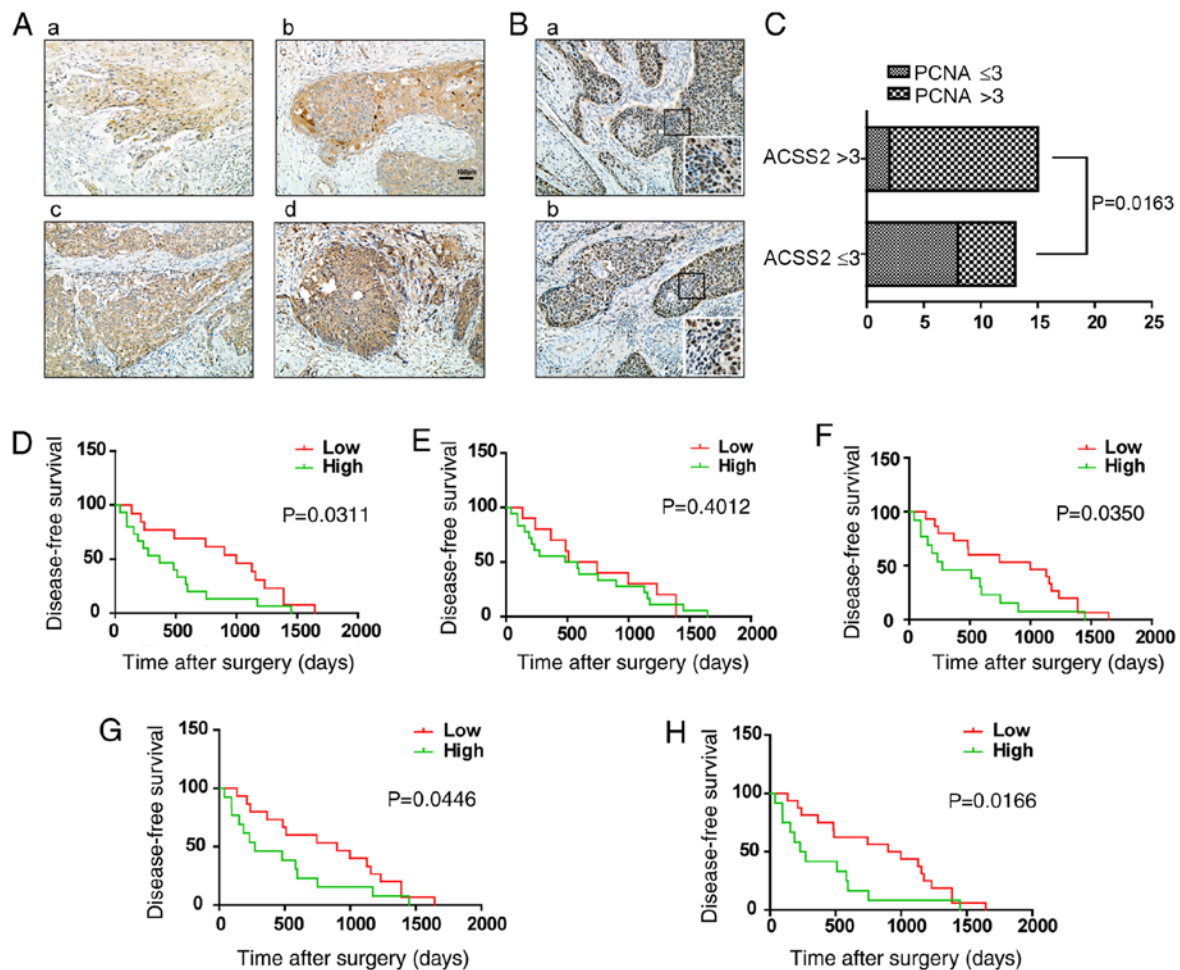


Figure 4. The prognostic value of ACSS2 and PCNA expression for patients with ESCC. (A) Representative images of IHC staining for ACSS2 in 28 pairs of human esophageal cancer tissues. Magnification, x200. (a) Weak ACSS2 expression in cancer tissue is scored as one point. (b) Moderate ACSS2 expression in cancer tissue is scored as two points. (c) Strong ACSS2 expression in cancer tissue is scored as three points. (d) Very strong ACSS2 expression in cancer tissue is scored as four points. (B) Representative images of IHC staining for PCNA in tumors. Magnification, x200. (a) High expression of PCNA. (b) Relatively low level of PCNA. The expression intensity of PCNA is shown in the magnified image (insert). Magnification, x400. (C) The association between ACSS2 and PCNA IHC staining intensity is presented as a histogram (n=28, P<0.05). (D-F) Kaplan-Meier analysis of disease-free survival (DFS) of patients with esophageal cancer (n=28) based on ACSS2, PCNA and Ki-67 expression. (G and H) Kaplan-Meier estimates of DFS according to the combinations of ACSS2 and PCNA, ACSS2 and Ki-67 respectively. IHC, immunohistochemistry; ACSS2, acetyl-CoA synthetase short-chain family member 2; AMPK, AMP-activated protein kinase; PCNA, proliferating cell nuclear antigen.

p-AMPK showed a decreasing tendency, whereas there was no significant difference in p-ULK1, which mediates autophagy (Fig. 3E). Furthermore, the levels of PCNA and ACSS2 were significantly affected after dorsomorphin treatment, showing an even stronger inhibition of ACSS2 (Fig. 3F). These results indicated that the interaction of ACSS2 with AMPK signaling mediates the stabilization of PCNA and DNA repair.

*Combination of ACSS2 with PCNA expression generates a better predictive model for overall survival.* To explore the association between ACSS2 and ESCC development, we further examined the association of ACSS2 expression with the clinicopathological characteristics of ESCC patients. The results indicated that the level of ACSS2 was higher in ESCC tissues, than that in the adjacent normal tissues ( $3.23 \pm 0.55$  vs.  $1.56 \pm 1.36$ ; P<0.05, Figs. 1A and 4A). To determine the correlation of ACSS2 and PCNA expression, we analyzed samples from two independent cohorts of ESCC patients. An ACSS2 staining score >3 in the cohort was considered high, while a

score  $\leq 3$  in the cohort was considered low, and cohorts 1 and 2 included 15 and 13 patients, respectively. We found that the strong intensity of ACSS2 increased the expression of PCNA in ESCC tumors (Fig. 4B). However, the clinicopathological correlation analysis revealed no positive correlation between elevated ACSS2 levels and age, gender, tumor diameter, lymph node metastasis, TNM stage and differentiation. Notably, the expression of ACSS2 was higher in tumors with high PCNA expression compared to those with low PCNA expression (P=0.0163) and was higher in tumors with Ki-67 overexpression (P<0.01, Fig. 4C, Table I). Furthermore, to establish a more sensitive model for predicting the outcomes of patients with ESCC, we combined ACSS2 expression and PCNA or Ki-67 intensity to create a prognostic scoring system. Based on the IHC scores, the patients were stratified into two subgroups (Ki-67 and PCNA, respectively): A low subgroup for low IHC-positive rates or scores (<50% or  $\leq 3$ ) and a high subgroup for high IHC-positive rates or scores ( $\geq 50\%$  or >3). The analysis showed that the predictive value

of ACSS2 alone was higher than that of PCNA ( $P=0.0311$  vs.  $P=0.4012$ ; Fig. 4D and E), and a combination of ACSS2 and PCNA revealed a better prognostic value ( $P=0.0446$ ; Fig. 4G). In addition, the combination of Ki-67 and ACSS2 was better than that for Ki-67 or ACSS2 alone ( $P=0.0166$ ; Fig. 4F and H). These results suggest that the combination of ACSS2 and PCNA expression could establish a better predictive model for the overall survival of ESCC patients.

## Discussion

Due to its immortalized nature, tumor progression is restricted by an irregular and deficient vascular network that is characterized by hypoxia and nutrient deficiency. While a majority of tumor cells remain viable, these cells continue to cautiously proliferate and tend to develop resistance to current therapies, thereby permitting survival, repopulation and metastasis (48-50). Except for the limited blood supply in tumor-restricting drug distribution, the tumor cells in regions of limited nutrition are likely to be resistant to drugs. Moreover, increasing evidence reveals that nutrient stress can stimulate transcriptional amplification, leading to the increased expression of genes encoding proteins that cause drug resistance, including autophagy, DNA repair, cell cycle progression and multidrug-resistant transporters, through diverse pathways (51-53). An improved understanding of the mechanisms that provide resistance to nutrient stress may clarify the reasons for treatment failure in patients with cancer. Tumor cells located far from functional blood vessels may receive a low supply, thus serum starvation is a well-established approach for inducing a broad range of cellular stresses. In the present study, we observed the upregulation of ACSS2 when esophageal squamous cell carcinoma cells (ESCCs), but not normal cells, were exposed to limited serum for a short or long period of time. This finding led us to consider the underlying roles for ACSS2 in the coping strategy. In this study, ACSS2 expression was assessed in ESCC patients and higher expression of ACSS2 was found in tumors focused in core and cell-rich areas. Thus, identification of whether and how ACSS2 contributes to malignant behavior may provide new therapeutic opportunities for ESCC.

In the present study, it was demonstrated that ACSS2 knockdown caused less tolerance to serum deprivation in ESCCs. First, we observed ACSS2-dependent viability, and the expression of ACSS2 was more important when cells were cultured *in vitro* under limited nutrients. Notably, the level of ACSS2 may stabilize the transcription and translation of PCNA, especially under nutrient stress. PCNA executes its major function as a processivity factor in DNA replication by tethering replicative polymerases to a genomic template and as a central factor to control genome stability (2,54-57). In general, inhibition of proliferation also involves changes in the cell cycle. Our findings indicated that cells were arrested in the G2/M phase upon siRNA-ACSS2 treatment. The DNA damage checkpoint at G2/M is important for DNA repair; thus, its dysfunction leads to apoptosis or death. In combination with cisplatin, pretreatment with siRNA-ACSS2 could cause apoptosis and death, which have marked synergistic effects. The expression of ACSS2 links nutrient intake and stress signaling with autophagy, tumor growth and metastasis (14,21,39,58).

Other groups have demonstrated higher ACSS2 expression in the bladder cancer patients with cisplatin resistance, suggesting that ACSS2 is involved in lipid metabolic alterations (24,59). Together with our findings, these data support the proposition that nutrient stress-induced ACSS2 upregulation may function protectively to maintain proliferation and prevent apoptosis.

Many tumors exhibit deregulated AMPK activity, which regulates energy homeostasis and autophagy and in turn requires increased amounts of carbon sources, such as acetate, glucose and fatty acids, to meet the needs of reprogrammed anabolic metabolism (28-30,39). Indeed, reprogramming energy metabolism is an emerging hallmark of many cancers as adjusting energy metabolism is essential to fuel cell growth and division. Acetyl-CoA represents a central node of carbon metabolism that plays a particular role in the bioenergetics, cell proliferation, and the regulation of gene expression. ACSS2 is the key factor that enables cells to maximally utilize acetate and produce acetyl-CoA for the synthesis of fatty acids and sterols and the modification of histones (14,39). Our results demonstrated that ACSS2 sufficiently protects cancer cells from cisplatin, specifically, which directly regulates the stabilization and expression of PCNA during DNA repair. Another group demonstrated that glucose deprivation results in AMPK-mediated ACSS2 phosphorylation and nuclear translocation, which promote lysosomal biogenesis, autophagy, survival, and tumorigenesis (39). We also observed that under nutrient stress, ESCCs exhibited an accumulation of p-AMPK. In particular, previous studies have shown that ACSS2 also promotes carcinogenesis by increasing the expression of autophagy-related factors, such as LAMP1, LC3B, and ATG3 (39,60). Furthermore, activated AMPK induced by nutrient stress directly phosphorylates ULK1, a serine/threonine kinase, which is necessary for the formation of autophagosomes (61). In contrast to the activation of AMPK, our results found no significant changes in either p-ULK1 or ULK by siRNA-ACSS2 or nutrient stress treatment in ESCCs. Interestingly, the inhibition of AMPK signaling with dorsomorphin also led to the downregulation of ACSS2, which was even more obvious than that of PCNA, suggesting that an interaction between ACSS2 and AMPK signaling ensures the survival and further resistance of ESCCs. The clinical significance of ACSS2 in ESCC has been presented in our study, although known prognostic factors, such as tumor grade, differentiation and lymph node metastasis, fail to be significant in the analysis. However, we found a positive correlation between the expression of ACSS2 and PCNA or Ki-67, suggesting its potential prognostic value. Although the prognostic relevance of ACSS2 in ESCC needs to be confirmed with larger-scale clinicopathologic analyses, at the least, our study has identified aberrant expression of ACSS2 as an independent prognostic factor in our small samples, and ACSS2 expression could be integrated with PCNA to generate a better risk stratification for ESCC patients.

Altogether, PCNA plays a dual role in replication and DNA repair under nutrient stress in ESCC. By creating an environment of nutrient stress, we showed here that PCNA is crucial to manage DNA damage, to complete efficient DSB repair, and to survive. Furthermore, ACSS2 cooperated with AMPK pathway activity to regulate the expression of PCNA, especially under nutrient stress. Finally, it was demonstrated that the combination of ACSS2 and PCNA expression could

establish a better predictive model for the survival of ESCC patients.

### Acknowledgements

Not applicable.

### Funding

The current study was supported by the National Natural Science Foundation of China (grant no. 81572956), the Jiangsu Provincial Science and Technology Supporting Program (grant no. BE2017096), the Medical Innovation Team of Jiangsu Province (grant no. CXTDC2016009) and the Student Innovation Training Program Projects of Jiangsu University (grant no. 201810299262W).

### Availability of data and materials

The datasets used and/or during the present study are available from the corresponding author on reasonable request.

### Authors' contributions

YZ, DC and CM conceived and designed the study. LM, YZ, DW, QT, XW, HZ, XG, JW, RL and JD performed the experiments. YZ and DC wrote the paper. YZ, CM, XW and DC reviewed and edited the manuscript. All authors read and approved the manuscript and agree to be accountable for all aspects of the research in ensuring that the accuracy or integrity of any part of the work are appropriately investigated and resolved.

### Ethics approval and consent to participate

The Ethics Committee of the Affiliated Hospital of Jiangsu University approved the research. All methods, including the collection and use of patient samples, were performed in accordance with the relevant guidelines and regulations and all patients provided signed informed consent.

### Patient consent for publication

Not applicable.

### Competing interests

The authors declare that they have no competing interests.

### References

- Choe KN and Moldovan GL: Forging ahead through darkness: PCNA, Still the principal conductor at the replication fork. *Mol Cell* 65: 380-392, 2017.
- De March M and De Biasio A: The dark side of the ring: Role of the DNA sliding surface of PCNA. *Crit Rev Biochem Mol Biol* 52: 663-673, 2017.
- Gu L, Lingeman R, Yakushijin F, Sun E, Cui Q, Chao J, Hu W, Li H, Hickey RJ, Stark JM, *et al*: The anticancer activity of a First-in-class Small-molecule targeting PCNA. *Clin Cancer Res* 24: 6053-6065, 2018.
- Shiomi Y and Nishitani H: Control of genome integrity by RFC complexes; conductors of PCNA loading onto and unloading from chromatin during DNA Replication. *Genes* 8: pii: E52, 2017.
- Tan Z, Wortman M, Dillehay KL, Seibel WL, Evelyn CR, Smith SJ, Malkas LH, Zheng Y, Lu S and Dong Z: Small-molecule targeting of proliferating cell nuclear antigen chromatin association inhibits tumor cell growth. *Mol Pharmacol* 81: 811-819, 2012.
- Bartová E, Suchanková J, Legartová S, Malýšková B, Hornáček M, Skalníková M, Mašata M, Raška I and Kozubek S: PCNA is recruited to irradiated chromatin in late S-phase and is most pronounced in G2 phase of the cell cycle. *Protoplasma* 254: 2035-2043, 2017.
- Recouvreur MV and Comisso C: Macropinocytosis: A metabolic adaptation to nutrient stress in cancer. *Front Endocrinol (Lausanne)* 8: 261, 2017.
- White E, Mehnert JM and Chan CS: Autophagy, metabolism, and cancer. *Clin Cancer Res* 21: 5037-5046, 2015.
- Peck B, Ferber EC and Schulze A: Antagonism between FOXO and MYC regulates cellular powerhouse. *Front Oncol* 3: 96, 2013.
- Singh D, Arora R, Kaur P, Singh B, Mannan R and Arora S: Overexpression of hypoxia-inducible factor and metabolic pathways: Possible targets of cancer. *Cell Biosci* 7: 62, 2017.
- El Hout M, Dos Santos L, Hamai A and Mehrpour M: A promising new approach to cancer therapy: Targeting iron metabolism in cancer stem cells. *Semin Cancer Biol* 53: 125-138, 2018.
- Conacci-Sorrell M, Ngouenet C, Anderson S, Brabletz T and Eisenman RN: Stress-induced cleavage of Myc promotes cancer cell survival. *Genes Dev* 28: 689-707, 2014.
- Hu G, Zhou Y, Zhu Y, Zhou L, Ling R, Wu D, Mi L, Wang X, Dai D, Mao C and Chen D: Novel transduction of nutrient stress to Notch pathway by RasGRP3 promotes malignant aggressiveness in human esophageal squamous cell carcinoma. *Oncol Rep* 38: 2975-2984, 2017.
- Chen R, Xu M, Nagati J and Garcia JA: Coordinate regulation of stress signaling and epigenetic events by Acss2 and HIF-2 in cancer cells. *PLoS One* 12: e0190241, 2017.
- Keenan MM and Chi JT: Alternative fuels for cancer cells. *Cancer J* 21: 49-55, 2015.
- Lakhter AJ, Hamilton J, Konger RL, Brustovetsky N, Broxmeyer HE and Naidu SR: Glucose-independent acetate metabolism promotes melanoma cell survival and tumor growth. *J Biol Chem* 291: 21869-21879, 2016.
- Vysochan A, Sengupta A, Weljie AM, Alwine JC and Yu Y: ACSS2-mediated acetyl-CoA synthesis from acetate is necessary for human cytomegalovirus infection. *Proc Natl Acad Sci USA* 114: E1528-E1535, 2017.
- Cao TT, Lin SH, Fu L, Tang Z, Che CM, Zhang LY, Ming XY, Liu TF, Tang XM, Tan BB, *et al*: Eukaryotic translation initiation factor 5A2 promotes metabolic reprogramming in hepatocellular carcinoma cells. *Carcinogenesis* 38: 94-104, 2017.
- Comerford SA, Huang Z, Du X, Wang Y, Cai L, Witkiewicz AK, Walters H, Tantawy MN, Fu A, Manning HC, *et al*: Acetate dependence of tumors. *Cell* 159: 1591-1602, 2014.
- Schug ZT, Vande Voorde J and Gottlieb E: The metabolic fate of acetate in cancer. *Nat Rev Cancer* 16: 708-717, 2016.
- Zhang S, He J, Jia Z, Yan Z and Yang J: Acetyl-CoA synthetase 2 enhances tumorigenesis and is indicative of a poor prognosis for patients with renal cell carcinoma. *Urol Oncol* 36: 243.e9-243.e20, 2018.
- Sun L, Kong Y, Cao M, Zhou H, Li H, Cui Y, Fang F, Zhang W, Li J, Zhu X, *et al*: Decreased expression of acetyl-CoA synthase 2 promotes metastasis and predicts poor prognosis in hepatocellular carcinoma. *Cancer Sci* 108: 1338-1346, 2017.
- Bae JM, Kim JH, Oh HJ, Park HE, Lee TH, Cho NY and Kang GH: Downregulation of acetyl-CoA synthetase 2 is a metabolic hallmark of tumor progression and aggressiveness in colorectal carcinoma. *Mod Pathol* 30: 267-277, 2017.
- Lee MY, Yeon A, Shahid M, Cho E, Sairam V, Figlin R, Kim KH and Kim J: Reprogrammed lipid metabolism in bladder cancer with cisplatin resistance. *Oncotarget* 9: 13231-13243, 2018.
- Dauer P, Nomura A, Saluja A and Banerjee S: Microenvironment in determining chemo-resistance in pancreatic cancer: Neighborhood matters. *Pancreatol* 17: 7-12, 2017.
- Chou CW, Wang CC, Wu CP, Lin YJ, Lee YC, Cheng YW and Hsieh CH: Tumor cycling hypoxia induces chemoresistance in glioblastoma multiforme by upregulating the expression and function of ABCB1. *Neuro Oncol* 14: 1227-1238, 2012.
- Iyama T and Wilson DM III: DNA repair mechanisms in dividing and non-dividing cells. *DNA Repair (Amst)* 12: 620-636, 2013.
- Yung MM, Ngan HY and Chan DW: Targeting AMPK signaling in combating ovarian cancers: Opportunities and challenges. *Acta Biochim Biophys Sin (Shanghai)* 48: 301-317, 2016.

29. Zeng J, Liu W, Fan YZ, He DL and Li L: PrLZ increases prostate cancer docetaxel resistance by inhibiting LKB1/AMPK-mediated autophagy. *Theranostics* 8: 109-123, 2018.
30. Oh TI, Lee JH, Kim S, Nam TJ, Kim YS, Kim BM, Yim WJ and Lim JH: Fascaplysin sensitizes anti-cancer effects of drugs targeting AKT and AMPK. *Molecules* 23: pii: E42, 2017.
31. Pan Y, Zhang F, Zhao Y, Shao D, Zheng X, Chen Y, He K, Li J and Chen L: Berberine enhances chemosensitivity and induces apoptosis through Dose-orchestrated AMPK signaling in breast cancer. *J Cancer* 8: 1679-1689, 2017.
32. Lam TG, Jeong YS, Kim SA and Ahn SG: New metformin derivative HL156A prevents oral cancer progression by inhibiting the insulin-like growth factor/AKT/mammalian target of rapamycin pathways. *Cancer Sci* 109: 699-709, 2018.
33. Pan Y, Liu L, Li S, Wang K, Ke R, Shi W, Wang J, Yan X, Zhang Q, Wang Q, *et al*: Activation of AMPK inhibits TGF- $\beta$ 1-induced airway smooth muscle cells proliferation and its potential mechanisms. *Sci Rep* 8: 3624, 2018.
34. Liu L, Pan Y, Song Y, Su X, Ke R, Yang L, Gao L and Li M: Activation of AMPK  $\alpha$ 2 inhibits airway smooth muscle cells proliferation. *Eur J Pharmacol* 791: 235-243, 2016.
35. Zhao Y, Liu Y, Jing Z, Peng L, Jin P, Lin Y, Zhou Y, Yang L, Ren J, Xie Q and Jin X: N-oleoylethanolamide suppresses intimal hyperplasia after balloon injury in rats through AMPK/PPAR $\alpha$  pathway. *Biochem Biophys Res Commun* 496: 415-421, 2018.
36. Zhang T, Guo P, Zhang Y, Xiong H, Yu X, Xu S, Wang X, He D and Jin X: The antidiabetic drug metformin inhibits the proliferation of bladder cancer cells in vitro and in vivo. *Int J Mol Sci* 14: 24603-24618, 2013.
37. Feng J, Qi B, Guo L, Chen LY, Wei XF, Liu YZ and Zhao BS: miR-382 functions as a tumor suppressor against esophageal squamous cell carcinoma. *World J Gastroenterol* 23: 4243-4251, 2017.
38. Livak KJ and Schmittgen TD: Analysis of relative gene expression data using real-time quantitative PCR and the 2(-Delta Delta C(T)) method. *Methods* 25: 402-408, 2001.
39. Li X, Yu W, Qian X, Xia Y, Zheng Y, Lee JH, Li W, Lyu J, Rao G, Zhang X, *et al*: Nucleus-translocated ACS2 promotes gene transcription for lysosomal biogenesis and autophagy. *Mol Cell* 66: 684-697.e9, 2017.
40. Schug ZT, Peck B, Jones DT, Zhang Q, Grosskurth S, Alam IS, Goodwin LM, Smethurst E, Mason S, Blyth K, *et al*: Acetyl-CoA synthetase 2 promotes acetate utilization and maintains cancer cell growth under metabolic stress. *Cancer Cell* 27: 57-71, 2015.
41. Zhang L, Cheng X, Gao Y, Bao J, Guan H, Lu R, Yu H, Xu Q and Sun Y: Induction of ROS-independent DNA damage by curcumin leads to G2/M cell cycle arrest and apoptosis in human papillary thyroid carcinoma BCPAP cells. *Food Funct* 7: 315-325, 2016.
42. Huang HW, Tang JY, Ou-Yang F, Wang HR, Guan PY, Huang CY, Chen CY, Hou MF, Sheu JH and Chang HW: Sinularin selectively kills breast cancer cells showing G2/M arrest, apoptosis, and oxidative DNA damage. *Molecules* 23: pii: E849, 2018.
43. Hegde M, Vartak SV, Kavitha CV, Ananda H, Prasanna DS, Gopalakrishnan V, Choudhary B, Rangappa KS and Raghavan SC: A benzothiazole derivative (5g) induces DNA damage and potent G2/M arrest in cancer cells. *Sci Rep* 7: 2533, 2017.
44. Finzel A, Grybowski A, Strasen J, Cristiano E and Loewer A: Hyperactivation of ATM upon DNA-PKcs inhibition modulates p53 dynamics and cell fate in response to DNA damage. *Mol Biol Cell* 27: 2360-2367, 2016.
45. Tomimatsu N, Mukherjee B and Burma S: Distinct roles of ATR and DNA-PKcs in triggering DNA damage responses in ATM-deficient cells. *EMBO Rep* 10: 629-635, 2009.
46. Shen B, He PJ and Shao CL: Norcantharidin induced DU145 cell apoptosis through ROS-mediated mitochondrial dysfunction and energy depletion. *PLoS One* 8: e84610, 2013.
47. Bártová E, Malyšková B, Komůrková D, Legartová S, Suchánková J, Krejčí J and Kozubek S: Function of heterochromatin protein 1 during DNA repair. *Protoplasma* 254: 1233-1240, 2017.
48. Saggar JK, Yu M, Tan Q and Tannock IF: The tumor microenvironment and strategies to improve drug distribution. *Front Oncol* 3: 154, 2013.
49. Tan Q, Saggar JK, Yu M, Wang M and Tannock IF: Mechanisms of drug resistance related to the microenvironment of solid tumors and possible strategies to inhibit them. *Cancer J* 21: 254-262, 2015.
50. Rohwer N and Cramer T: Hypoxia-mediated drug resistance: Novel insights on the functional interaction of HIFs and cell death pathways. *Drug Resist Updat* 14: 191-201, 2011.
51. Ojha R, Bhattacharyya S and Singh SK: Autophagy in cancer stem cells: A potential link between chemoresistance, recurrence, and metastasis. *Biores Open Access* 4: 97-108, 2015.
52. Hua Y, Gorshkov K, Yang Y, Wang W, Zhang N and Hughes DP: Slow down to stay alive: HER4 protects against cellular stress and confers chemoresistance in neuroblastoma. *Cancer* 118: 5140-5154, 2012.
53. Salaroglio IC, Panada E, Moiso E, Buondonno I, Provero P, Rubinstein M, Kopecka J and Riganti C: PERK induces resistance to cell death elicited by endoplasmic reticulum stress and chemotherapy. *Mol Cancer* 16: 91, 2017.
54. Baserga R: Growth regulation of the PCNA gene. *J Cell Sci* 98: 433-436, 1991.
55. Feng W, Guo Y, Huang J, Deng Y, Zang J and Huen MS: TRAIIP regulates replication fork recovery and progression via PCNA. *Cell Discov* 2: 16016, 2016.
56. Fox JT, Lee KY and Myung K: Dynamic regulation of PCNA ubiquitylation/deubiquitylation. *FEBS Lett* 585: 2780-2785, 2011.
57. Slade D: Maneuvers on PCNA rings during DNA replication and repair. *Genes (Basel)* 9: pii: E416, 2018.
58. Bidkhorji G, Benfeitas R, Klevstig M, Zhang C, Nielsen J, Uhlen M, Boren J and Mardinoglu A: Metabolic network-based stratification of hepatocellular carcinoma reveals three distinct tumor subtypes. *Proc Natl Acad Sci USA* 115: E11874-E11883, 2018.
59. Wen H, Lee S, Zhu WG, Lee OJ, Yun SJ, Kim J and Park S: Glucose-derived acetate and ACS2 as key players in cisplatin resistance in bladder cancer. *Biochim Biophys Acta Mol Cell Biol Lipids* 1864: 413-421, 2019.
60. Yao L, Guo X and Gui Y: Acetyl-CoA synthetase 2 promotes cell migration and invasion of renal cell carcinoma by upregulating lysosomal-associated membrane protein 1 expression. *Cell Physiol Biochem* 45: 984-992, 2018.
61. Puente C, Hendrickson RC and Jiang X: Nutrient-regulated phosphorylation of ATG13 inhibits starvation-induced autophagy. *J Biol Chem* 291: 6026-6035, 2016.